

## Development of the Double Cascade Reconstruction Technique in the Baikal-GVD Neutrino Telescope

V.A. Allakhverdyan,<sup>a</sup> A.D. Avrorin,<sup>b</sup> A.V. Avrorin,<sup>b</sup> V.M. Aynutdinov,<sup>b</sup> Z. Bardačová,<sup>d</sup> I.A. Belolaptikov,<sup>a</sup> I.V. Borina,<sup>a</sup> N.M. Budnev,<sup>e</sup> V.Y. Dik,<sup>a,j</sup> G.V. Domogatsky,<sup>b</sup> A.A. Doroshenko,<sup>b</sup> R. Dvornický,<sup>d</sup> A.N. Dyachok,<sup>e</sup> Zh.-A.M. Dzhilkibaev,<sup>b</sup> E. Eckerová,<sup>d,\*</sup> T.V. Elzhov,<sup>a</sup> L. Fajt,<sup>f</sup> A.R. Gafarov,<sup>e</sup> K.V. Golubkov,<sup>b</sup> N.S. Gorshkov,<sup>a</sup> T.I. Gress,<sup>e</sup> K.G. Kebkal,<sup>c</sup> O.G. Kebkal,<sup>c</sup> A. Khatun,<sup>d</sup> E.V. Khramov,<sup>a</sup> M.M. Kolbin,<sup>a</sup> K.V. Konischev,<sup>a</sup> A.V. Korobchenko,<sup>a</sup> A.P. Koshechkin,<sup>b</sup> V.A. Kozhin,<sup>h</sup> M.V. Kruglov,<sup>a</sup> V.F. Kulepov,<sup>g</sup> Y.M. Malyshkin,<sup>a</sup> M.B. Milenin,<sup>b</sup> R.R. Mirgazov,<sup>e</sup> D.V. Naumov,<sup>a</sup> V. Nazari,<sup>a</sup> D.P. Petukhov,<sup>b</sup> E.N. Pliskovsky,<sup>a</sup> M.I. Rozanov,<sup>i</sup> V.D. Rushay,<sup>a</sup> E.V. Ryabov,<sup>e</sup> G.B. Safronov,<sup>b</sup> D. Seitova,<sup>a,j</sup> B.A. Shaybonov,<sup>a</sup> M.D. Shelepov,<sup>b</sup> F. Šimkovic,<sup>d,f</sup> A.E. Sirenko,<sup>a</sup> A.V. Skurikhin,<sup>h</sup> A.G. Solovjev,<sup>a</sup> M.N. Sorokovikov,<sup>a</sup> I. Štekl,<sup>f</sup> A.P. Stromakov,<sup>b</sup> O.V. Suvorova,<sup>b</sup> V.A. Tabolenko,<sup>e</sup> Y.V. Yablokova<sup>a</sup> and D.N. Zaborov<sup>b</sup>

<sup>a</sup>Joint Institute for Nuclear Research, Dubna, Russia

<sup>b</sup>Institute for Nuclear Research, Russian Academy of Sciences, Moscow, Russia

<sup>c</sup>EvoLogics GmbH, Berlin, Germany

<sup>d</sup>Comenius University, Bratislava, Slovakia

<sup>e</sup>Irkutsk State University, Irkutsk, Russia

<sup>f</sup>Czech Technical University in Prague, Prague, Czech Republic

<sup>g</sup>Nizhny Novgorod State Technical University, Nizhny Novgorod, Russia

<sup>h</sup>Skobeltsyn Institute of Nuclear Physics, Moscow State University, Moscow, Russia

<sup>i</sup>St. Petersburg State Marine Technical University, St.Petersburg, Russia

<sup>j</sup>Institute for Nuclear Physics ME RK, Almaty, 050032 Kazakhstan

E-mail: [eliska.eckerova@fmph.uniba.sk](mailto:eliska.eckerova@fmph.uniba.sk)

Baikal-GVD is a cubic kilometer scale neutrino telescope being constructed in Lake Baikal. In 2022 it consists of 2880 optical modules attached to 80 vertical strings. Detection of neutrinos is based on detection of the Cherenkov radiation emitted by the products of neutrino interactions. In this contribution, development of the double cascade reconstruction technique is described. The first event rate estimation from Monte Carlo simulations of tau neutrino double cascade events as well as the background event rates are presented.

\*\*\* 27th European Cosmic Ray Symposium - ECRS \*\*\*

\*\*\* 25-29 July 2022 \*\*\*

\*\*\* Nijmegen, the Netherlands \*\*\*

---

\*Speaker

## 1. Introduction

The Baikal Gigaton Volume Detector (Baikal-GVD) [1] is a cubic kilometer scale neutrino telescope under construction in the deepest freshwater lake in the world – Lake Baikal. It is located in depths of approximately 750 - 1275 m and  $\sim 3 - 4$  km from shore. The main aim of the Baikal-GVD is to observe astrophysical neutrinos via detection of the Cherenkov radiation emitted by the products of neutrino interactions.

An independent structural unit of the Baikal-GVD is a cluster. The cluster consists of 8 vertical strings arranged in heptagonal structure – one central string and seven peripheral strings separated by 60 m from the cluster center. Spacing between the central strings of two neighboring clusters is approximately 300 m, see Fig. 1a. There are 36 Optical Modules (OM) installed on every string, see Fig. 1b. Distance between two neighboring OMs is 15 m. The OM components are housed in a pressure resistant glass sphere with a diameter of 42 cm. The main component of the OM is a 10" photomultiplier tube. As of April 2022, Baikal-GVD consists of 10 clusters, resulting in 80 strings and 2880 OMs deployed.

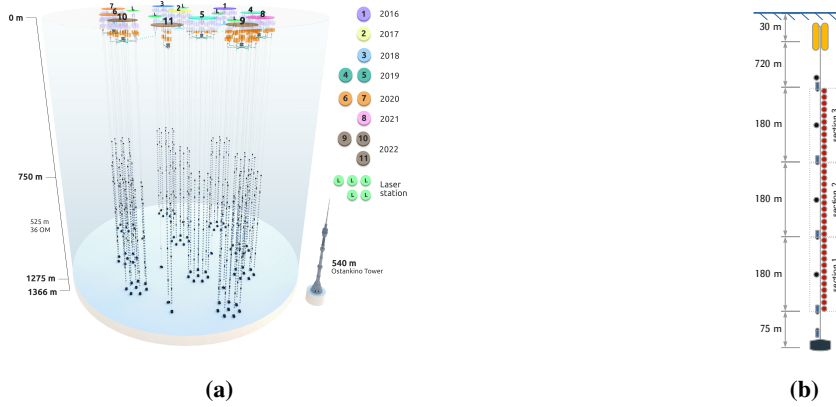


**Figure 1:** a) Scheme of the Baikal-GVD telescope in 2022. There are 10 clusters completely installed. b) Design of the string of the Baikal-GVD telescope.

There are two basic types of Cherenkov light signatures in the Baikal-GVD – tracks and cascades. In neutral current (NC) and charged current (CC) neutrino interactions a hadronic cascade is created. In addition, in CC interaction of neutrino a lepton with flavor corresponding to the flavor of interacting neutrino is produced. In the case of electron neutrino, an electron is produced which starts an electromagnetic cascade. A muon originating in CC interaction of muon neutrino is observed as a track-like event. Tau lepton has relatively short lifetime so it can decay in the detector instrumented volume. When tau lepton decays into electron or hadrons then a second, electromagnetic or hadronic cascade is created in addition to the hadronic cascade initiated directly at the tau neutrino interaction vertex. As a consequence, a potentially observable double cascade signature is created in the detector.

Identification of  $\nu_\tau$  interaction is considered to be a promising method for observation of astrophysical neutrinos because  $\nu_\tau$  are nearly absent in the atmospheric neutrino flux (at TeV-PeV energies) [2]. Therefore, if  $\nu_\tau$  is detected, there is a very high probability that this neutrino is of astrophysical origin. In this paper, development of the double cascade reconstruction technique is presented.

## 2. Double Cascade Reconstruction Algorithm

Current version of the single cluster double cascade reconstruction algorithm consists of four main parts:

1. Hit selection
2. Hit sorting
3. Position and time reconstruction
4. Energy reconstruction

Described algorithm represents further steps in the development of the double cascade reconstruction algorithm published in [3].

### 2.1 Hit selection

The first step in the double cascade reconstruction algorithm is to suppress noise hits and select signal pulses for further steps of the reconstruction. Firstly, the pulse with the highest charge is tagged as a reference pulse. Subsequent pulses are chosen according to the criterion:

$$|T^{ref} - T_i^{meas}| < d_i/v + \delta t, \quad (1)$$

where  $T^{ref}$  is time of detection of the reference pulse,  $T_i^{meas}$  is detection time of studied pulse,  $d_i$  is distance between OMs of the two considered pulses,  $v$  is the speed of light in water, and  $\delta t$  determines strictness of the criterion. For a pulse to be selected, there is an additional criterion: one of the neighboring OMs (two above or two below) has to detect a pulse in a certain time window (typically  $\sim 100$  ns). With  $\delta t$  set on 80 ns the mean signal pulse selection efficiency is at the level of 79 % and mean purity is approximately 99 %.

### 2.2 Hit sorting

The main aim of the second step of the double cascade reconstruction algorithm is to divide the set of pulses selected in the first step of the algorithm into two subsets that correspond to the two cascades. Selection of the subsets of the pulses is based on the first estimation of the positions and times of both cascades.

The idea is to select several sets of five pulses and to estimate the position and time of cascade for each of them. Particularly, the estimation of the cascade position and time is achieved by solving a set of equations for distances  $d_i$  between cascade vertex and the OMs that registered the pulses in the set:

$$d_i = \sqrt{(x - x_i)^2 + (y - y_i)^2 + (z - z_i)^2} = c/n(t - t_i), \quad (2)$$

where  $\mathbf{x} = (x, y, z, t)$  marks the space-time position of the cascade vertex,  $\mathbf{x}_i = (x_i, y_i, z_i, t_i)$  denotes the space-time coordinates of the particular pulse detected on the OM,  $c$  is the speed of light, and  $n$  is refractive index of water. The number of pulses (five) in the set was chosen as the lowest number of pulses required to determine  $\mathbf{x}$  unambiguously with this method [4]. Such a low number of selected pulses in these sets was chosen because it is more likely that these pulses correspond to one cascade only. If the selected set of five pulses consists of pulses that correspond to one cascade only, position and time of the cascade will be estimated accurately, see Fig. 2a. They are estimated inaccurately in the case when these five pulses correspond to both cascades or noise pulses, see

Fig. 2b. Assuming two cascades in an event and estimating positions and times of the cascade vertices from all possible sets of five pulses, two peaks that correspond to the two cascade vertices are expected to be produced from these position and time estimations. These peaks are identified and the first position  $\vec{R}$  and time  $T$  estimations of the two cascade vertices are thus obtained.

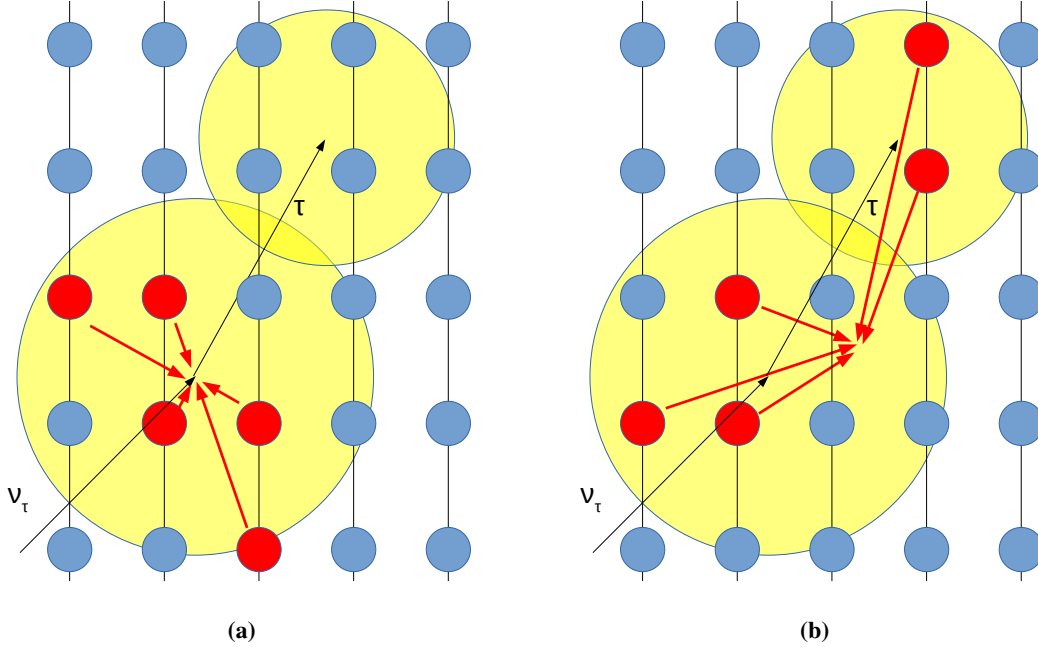


**Figure 2:** Illustration of the result of the position estimation from five pulses. a) All five pulses are from one cascade only, i.e. accurate estimation of cascade position. b) Set of five pulses consists of pulses from both cascades, i.e. inaccurate position estimation.

Application of this method on one simulated event is shown in Fig. 3. In this case, all sets of five pulses were used for estimation of position and time of cascade. From all estimations two peaks that correspond to two cascade vertices were created, for XZ plane see Fig. 3a, and for XY plane see Fig. 3b.

Subsequently, two subsets of pulses are created by selecting hits that correspond to the first estimation of positions and times of cascades according to the condition:

$$|T_i^{meas} - T_i^{exp}(\vec{R}, T)| \lesssim \delta T, \quad (3)$$

where  $T_i^{meas}$  is measured time of the pulse,  $T_i^{exp}$  is expected time of the pulse calculated with respect to the estimated time  $T$  and position  $\vec{R}$  of the cascade vertex, and  $\delta T$  determines stringency of the criterion. Every pulse can participate in one subset only.

Estimation of times and positions of cascades is computationally very extensive, if all sets of five pulses are used. Therefore, a reduced technique which uses only a few sets of five pulses for the estimation of positions and times of cascades is implemented in the reconstruction algorithm. Pulses are sorted according to their charge (from the highest to the lowest). The sorting of pulses increases probability that the position and time estimations of the two cascade vertices (two peaks in Fig. 3) can be identified only from several sets of five pulses.

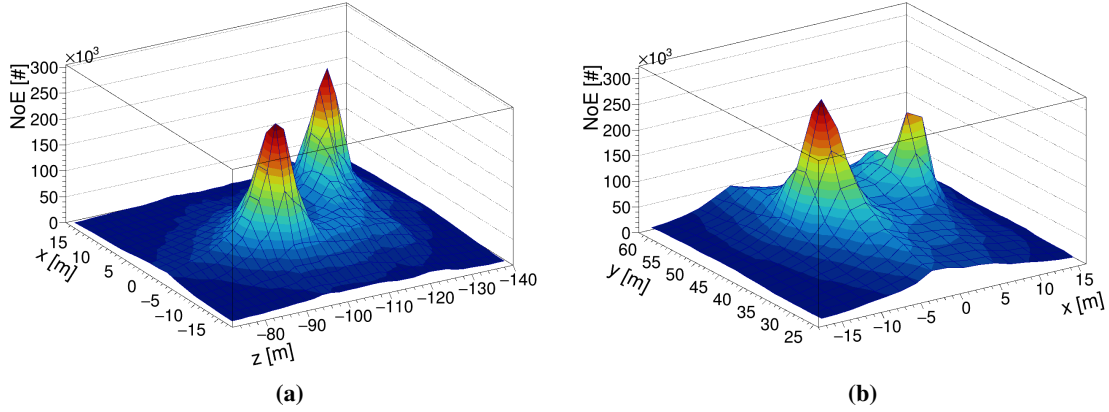


**Figure 3:** Result of the position estimation procedure, all sets of five pulses used. From all position estimations two peaks that correspond to the two cascade vertices were created. The simulated position of  $\nu_\tau$  cascade is [9, 47, -126], and  $\tau$  cascade simulated position is [-3, 45, -100]. a) XZ plane. b) XY plane.

### 2.3 Position and time reconstruction

In the third step of the double cascade reconstruction algorithm, the final estimated values for positions and times of cascade vertices are obtained. Input to this step of the algorithm are two subsets of pulses that correspond to the two cascades in double cascade event.

Positions and times of cascade vertices are estimated by a minimization of  $\chi^2$  distribution:

$$\chi^2 = \frac{1}{N_{hit1} + N_{hit2} - 7} \left( \sum_{i=0}^{N_{hit1}} \frac{(T_{1i}^{meas} - T_{1i}^{exp}(\vec{R}_1, T_1))^2}{\sigma_t^2} + \sum_{i=0}^{N_{hit2}} \frac{(T_{2i}^{meas} - T_{2i}^{exp}(\vec{R}_2, T_2))^2}{\sigma_t^2} \right), \quad (4)$$

where  $N_{hit1}$ ,  $N_{hit2}$  are number of pulses in subsets of hits corresponding to the two cascades,  $T_{1i}^{meas}$ ,  $T_{2i}^{meas}$  are times of detection of pulses from the subsets on  $i^{th}$  OM,  $T_{1i}^{exp}$ ,  $T_{2i}^{exp}$  are expected times of pulse detection on  $i^{th}$  OM, calculated with respect to the positions and times of the cascades –  $\vec{R}_1, T_1$  and  $\vec{R}_2, T_2$ , and  $\sigma_t$  is uncertainty in the measurement of time [5]. The direction of the double cascade event is defined as the vector between the reconstructed cascade vertices, therefore it is also obtained in this step.

### 2.4 Energy reconstruction

For reconstruction of energies of both cascades a minimization of log-likelihood function is used. The log-likelihood function is defined by the following formula:

$$L = - \sum_{i=0}^{hitOM} \log(P_i(q_i | Q_i)) - \sum_{i=0}^{unhitOM} \log(P_i(q_i = 0 | Q_i)), \quad (5)$$

where  $P_i(q_i | Q_i)$  represents the probability of observing charge  $q_i$  on  $i^{th}$  OM, while charge  $Q_i$  is expected. The expected charge on  $i^{th}$  OM is calculated as a sum of the charges expected from both cascades – taking into account position and orientation of the OM, reconstructed positions and directions of the cascades, and energies of the cascades [5].

### 3. Performance

To assess the precision of the double cascade reconstruction algorithm, Monte Carlo (MC) simulations of  $\nu_\tau$  double cascade events were used. An approximation of the neutrino flux given as  $\phi(E) = 2 \cdot 10^{-8} \cdot \left(\frac{E}{\text{GeV}}\right)^{-2} \text{GeV}^{-1} \text{s}^{-1} \text{sr}^{-1} \text{cm}^{-2}$  was considered in our preliminary studies. In the following we used a subset of simulated  $\nu_\tau$  events (so-called Double Cascade-like or DC-like events). The main criteria we applied are  $E_{\nu_\tau} > 100 \text{ TeV}$  and the distance between the cascade vertices larger than 10 m.

The precision with which the attributes of  $\nu_\tau$  double cascade events are reconstructed, namely the mean and median values of the distributions of mismatch between simulated and reconstructed values of the double cascade parameters is summarized in Tab. 1.

**Table 1:** Evaluation of the precision of the double cascade reconstruction algorithm. Mean and median values of the mismatch distributions between simulated  $x_{sim}$  and reconstructed  $x_{reco}$  values of various DC parameters are shown.

DC parameter	$ x_{sim} - x_{reco} $	
	mean	median
cascade A position [m]	3.09	2.27
cascade B position [m]	5.03	2.46
distance between vertices [m]	2.83	0.75
direction [deg]	9.96	2.67

The double cascade signature can also be created by other types of events for example atmospheric muon bundles. Multiple cascades can be produced along muon track, due to stochastic energy losses of muon. Additionally, other types of events can be misreconstructed as double cascade events. In following Tab. 2 expected rates of  $\nu_\tau$  double cascade like events and the background event rates before and after processing with the double cascade reconstruction algorithm as well as the efficiency of the algorithm are given.

**Table 2:** Efficiency of the double cascade reconstruction algorithm for various types of simulated events.  $NoE$  denotes expected number of events per cluster per year.  $NoE_{DCreco}$  means expected number of events that passed cuts in the double cascade reconstruction algorithm.

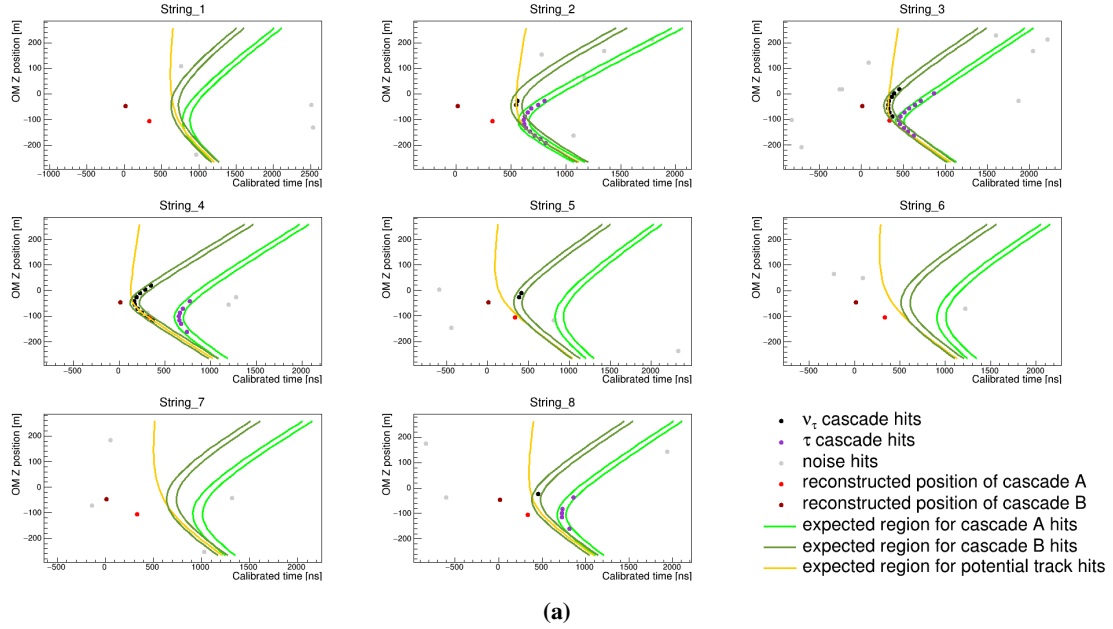
type of MC	$NoE$ [ $\text{y}^{-1} \text{cluster}^{-1}$ ]	$NoE_{DCreco}$ [ $\text{y}^{-1} \text{cluster}^{-1}$ ]	efficiency [%]
$\nu_\tau$ astrophysical (DC-like)*	$4.05 \cdot 10^{-2}$	$1.67 \cdot 10^{-2}$	41.3
atmospheric $\mu$ bundles	$5.38 \cdot 10^8$	38.1	$7.09 \cdot 10^{-6}$
$\nu_e$ atmospheric	9.34	$1.42 \cdot 10^{-3}$	$1.52 \cdot 10^{-2}$
$\nu_\mu$ atmospheric	87.4	$1.31 \cdot 10^{-2}$	$1.50 \cdot 10^{-2}$
$\nu_e$ astrophysical	1.71	$3.82 \cdot 10^{-2}$	2.24
$\nu_\mu$ astrophysical	$9.86 \cdot 10^{-1}$	$1.23 \cdot 10^{-2}$	1.25

\* signal MC

The visualization of one reconstructed  $\nu_\tau$  double cascade event from MC simulations is shown in Fig. 4a. In Fig. 4b one of the events identified as a potential double cascade event in experimental

data from year 2019 is displayed. On the second and third string exemplary double cascade pattern can be seen. However, on the fourth string there are hits located in the track expected region. Therefore, there is a high probability that this event is an atmospheric  $\mu$  bundle event.

## Baikal-GVD preliminary



## Baikal-GVD preliminary

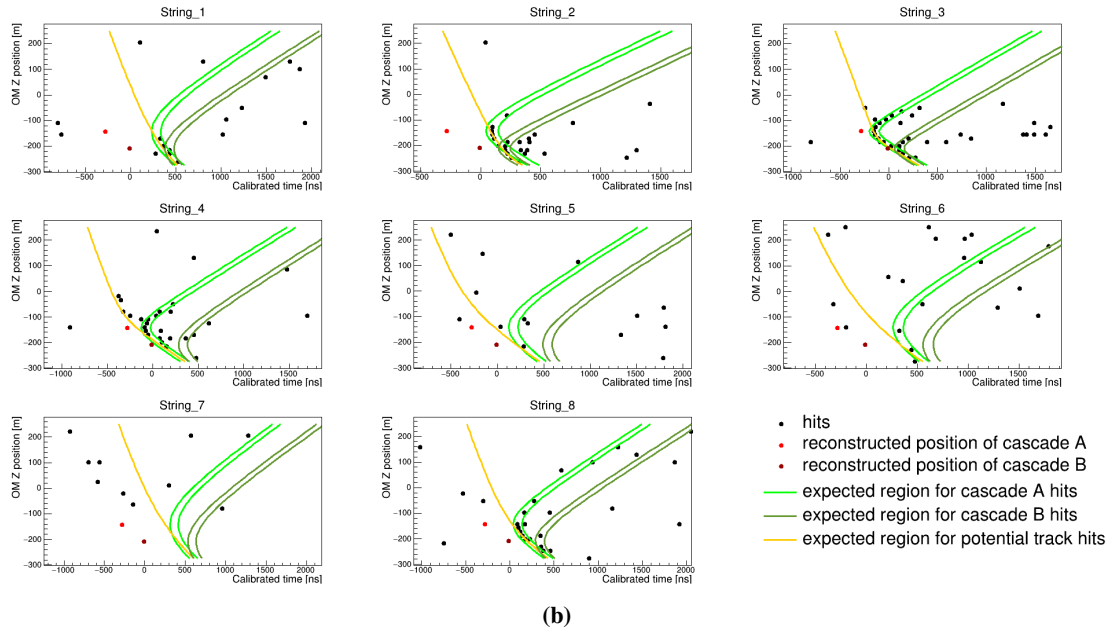


**Figure 4:** Visualizations of two events reconstructed by the double cascade reconstruction algorithm. For all eight strings in the cluster, dependence of the Z coordinate of the OM on time is displayed. a) Event from the MC simulations of  $\nu_\tau$ . b) Potential double cascade event identified in experimental data from year 2019.

## 4. Conclusion

In this article, recent development of the double cascade reconstruction algorithm was presented. The methods of estimation of the double cascade event attributes were described. The precision and efficiency of the algorithm as well as expected rates of signal and background events were given. The experimental data collected in year 2019 were processed with the double cascade reconstruction algorithm. A comparison of visualizations of one of the events reconstructed from MC simulations of  $\nu_\tau$  double cascade events with one of the potential double cascade events identified in experimental data was shown. The results presented in this paper are preliminary, there is an ongoing work on improvements of the efficiency and the precision of the algorithm.

## 5. Acknowledgments

This work is supported in the framework of the State project “Science” by the Ministry of Science and Higher Education of the Russian Federation under the contract 075-15-2020-778. We acknowledge support by the VEGA Grant Agency of the Slovak Republic under Contract No. 1/0607/20 and by the Ministry of Education, Youth and Sports of the Czech Republic under the INAFYM Grant No. CZ.02.1.01/0.0/0.0/16\_019/0000766. We also acknowledge the technical support of JINR staff for the computing facilities (JINR cloud).

## References

- [1] Baikal-GVD Collaboration: I.A. Belolaptikov et al., *Neutrino Telescope in Lake Baikal: Present and Nearest Future*, PoS ICRC2021 (2021), 002, doi: 10.22323/1.395.0002, arXiv:2109.14344 [astro-ph.HE].
- [2] A. Palladino et al., *The importance of observing astrophysical tau neutrinos*, J. Cosmol. Astropart. P. 8 (2018).
- [3] Baikal-GVD Collaboration: E. Eckerová et al., *Development of the Double Cascade Reconstruction Techniques in the Baikal-GVD Neutrino Telescope*, PoS ICRC2021 (2021), 1167, doi:10.22323/1.395.1167, arXiv:2108.00333 [astro-ph.IM].
- [4] B. Hartmann, *Reconstruction of Neutrino-Induced Hadronic and Electromagnetic Showers with the ANTARES Experiment*, PhD thesis, University Erlangen (2006), arXiv:astro-ph/0606697.
- [5] Baikal-GVD Collaboration: Zh.-A.M.Dzhilkibaev et al., *The Baikal-GVD neutrino telescope: search for high-energy cascades*, PoS ICRC2021 (2021), 1144, doi:10.22323/1.395.1144, arXiv:2108.01894 [astro-ph.HE].